Metallic Nanocomposites as Next-Generation Thermal Interface Materials

Preprint

Nirup Nagabandi, Cengiz Yegin, Jun K. Oh, and Mustafa Akbulut
Texas A&M University

Xuhui Feng, Charles King, and Sreekant Narumanchi
National Renewable Energy Laboratory

Presented at The Intersociety Conference on Thermal and Thermomechanical Phenomena in Electronic Systems (ITherm 2017) Conference
Orlando, Florida
May 30 – June 2, 2017

NREL is a national laboratory of the U.S. Department of Energy
Office of Energy Efficiency & Renewable Energy
Operated by the Alliance for Sustainable Energy, LLC

This report is available at no cost from the National Renewable Energy Laboratory (NREL) at www.nrel.gov/publications.

Conference Paper
NREL/CP-5400-68120
September 2017

Contract No. DE-AC36-08GO28308

NOTICE

This report is available at no cost from the National Renewable Energy Laboratory (NREL) at www.nrel.gov/publications.

Available electronically at SciTech Connect http:/www.osti.gov/scitech

Available for a processing fee to U.S. Department of Energy and its contractors, in paper, from:

U.S. Department of Energy
Office of Scientific and Technical Information
P.O. Box 62
Oak Ridge, TN 37831-0062
OSTI http://www.osti.gov
Phone: 865.576.8401
Fax: 865.576.5728
Email: reports@osti.gov

Available for sale to the public, in paper, from:

U.S. Department of Commerce
National Technical Information Service
5301 Shawnee Road
Alexandria, VA 22312
NTIS http://www.ntis.gov
Phone: 800.553.6847 or 703.605.6000
Fax: 703.605.6900
Email: orders@ntis.gov

Cover Photos by Dennis Schroeder: (left to right) NREL 26173, NREL 18302, NREL 19758, NREL 29642, NREL 19795.

NREL prints on paper that contains recycled content.

Metallic Nanocomposites as Next-Generation Thermal Interface Materials

Nirup Nagabandi[1], Cengiz Yegin[2], Xuhui Feng[3], Charles King[3], Jun Kyun Oh[2], Sreekant Narumanchi[3], Mustafa Akbulut[1, 2]
[1]Artie McFerrin Department of Chemical Engineering, Texas A&M University, 3122 TAMU College Station, TX 77843, USA
[2]Department of Materials Science and Engineering, Texas A&M University, 3003 TAMU, College Station, TX 77843, USA
[3]National Renewable Energy Laboratory (NREL), 15013 Denver West Parkway, Golden, CO 80401, USA
Email: makbulut@tamu.edu

ABSTRACT

Thermal interface materials (TIMs) are an integral and important part of thermal management in electronic devices. The electronic devices are becoming more compact and powerful. This increase in power processed or passing through the devices leads to higher heat fluxes and makes it a challenge to maintain temperatures at the optimal level during operation. Herein, we report a free standing nanocomposite TIM in which boron nitride nanosheets (BNNS) are uniformly dispersed in copper matrices *via* an organic linker, thiosemicarbazide. Integration of these metal-organic-inorganic nanocomposites was made possible by a novel electrodeposition technique where the functionalized BNNS (f-BNNS) experience the Brownian motion and reach the cathode through diffusion, while the nucleation and growth of the copper on the cathode occurs via the electrochemical reduction. Once the f-BNNS bearing carbonothioyl/thiol groups on the terminal edges come into the contact with copper crystals, the chemisorption reaction takes place. We performed thermal, mechanical, and structural characterization of these nanocomposites using scanning electron microcopy (SEM), diffusive laser flash (DLF) analysis, phase-sensitive transient thermoreflectence (PSTTR), and nanoindentation. The nanocomposites exhibited a thermal conductivity ranging from 211 W/mK to 277 W/mK at a filler mass loading of 0-12 wt.%. The nanocomposites also have about 4 times lower hardness as compared to copper, with values ranging from 0.27 GPa to 0.41 GPa. The structural characterization studies showed that most of the BNNS are localized at grain boundaries – which enable efficient thermal transport while making the material soft. PSTTR measurements revealed that the synergistic combinations of these properties yielded contact resistances on the order of 0.10 to 0.13 mm^{2}K/W, and the total thermal resistance of 0.38 to 0.56 mm^{2}K/W at bondline thicknesses of 30-50 µm. The coefficient of thermal expansion (CTE) of the nanocomposite is 11 ppm/K, which lies between the CTEs of aluminum (22 ppm/K) and silicon (3 ppm/K), which are common heat sink and heat source materials, respectively. The nanocomposite can also be deposited directly on to heat sink which will simplify the packaging processes by removing one possible element to assemble. These unique properties and ease of assembly makes the nanocomposite a promising next-generation TIM.

KEY WORDS:

TIM, Nanocomposite, Electrodeposition, Thermal Management, (Power) Electronics

NOMENCLATURE

TIM	Thermal interface materials
CTE	Coefficient of thermal expansion
BLT	Bondline thickness
BNNS	Boron nitride nanosheets
f-BNNS	Functionalized boron nitride nanosheets
TSC	Thiosemicarbazide
SEM	Scanning electron microscopy
DLF	Diffusive laser flash
PSTTR	Phase-sensitive transient thermoreflectance
TMA	Thermal mechanical analyzer
NMP	N-Methyl-2-Pyrrolidone
XPS	X-ray Photo Spectrometry
DSC	Differential Scanning Calorimetry
BN	Boron nitride
CPS	Counts per second

Greek Symbols

ρ	Mass density (kg/m^3)
α	Thermal diffusivity (m^2/s)
µm	Micrometer

INTRODUCTION

Conductive heat transfer is important for heat removal and thermal management in most electronic devices. Owing to the micro- and nano-scale roughness, two surfaces appearing in perfect contact at a macroscopic level are actually connected locally, only at the peaks of the surface asperities. This ineffective contact, resulting in thermal contact resistance, plays a major role in reducing the heat transported via mated surfaces. Also, thermal boundary resistance, which stems from the scattering of electrons and phonons due to sudden mismatch in materials, contributes to the inefficient heat transfer. Quantum confinement effects at micro and nano contacts result in the dispersion of phonons and electrons which further hinder the heat transfer across the boundary [1]. Thermal Interface Materials (TIMs) are often used to solve these problems. TIMs should be soft enough to either flow or conform to the asperities of the mating surfaces and should have high thermal conductivity to facilitate heat transfer and not to introduce any significant additional thermal resistance into the system.

Electronic industries are moving towards very compact device sizes and high performance, resulting in a large heat fluxes. Currently-available TIMs fail to facilitate very high thermal transport thus hindering the downsizing of devices and components. The immediate need to solve this problem is to develop next-generation TIMs, which possess very high thermal conductivity while maintaining acceptable mechanical properties relative to the present-day TIMs. The traditional approach to develop new TIMs has been to incorporate graphene, carbon nanotubes (CNT), graphene nanoparticles (GNP), and several other thermally conductive particles into soft matrices such as epoxy and silicone oil[2]–[6]. Solders are

another class of TIMs having thermal conductivities between 20 and 80 W/mK. However, these TIMs typically have a high coefficient of thermal expansion (CTE), which induce thermal stress and eventually lead to failures in devices, packages and components. This is due to the low CTE of silicon, 2.4 ppm/K, compared to that of indium, 29 ppm/K[7]. Across different classes of TIMs, the total thermal resistance is in the range of 1 to 30 mm^2K/W for bondline thicknesses (BLT) varying from 30-50 μm[8]. To satisfy the stringent needs of emerging power electronics, total thermal resistance of TIMs must reach values below 1 mm^2K/W. To accomplish this objective, we have relied on thermally conductive fillers and matrices; in particular - boron nitride nanosheets (BNNS) and copper matrix. Here, BNNS were selected as a filler owing to their low CTE, high thermal and chemical stability, and very high in-plane thermal conductivity[9], [10].

The chemical stability of BNNS helps in keeping the intrinsic properties intact but makes it difficult to disperse in a metal matrix. To introduce chemically inactive BNNS into the copper matrix, we functionalized BNNS with dual functional organic molecules (ligand) which can act as a bridge between BNNS and the copper matrix. We utilized thiosemicarbazide (TSC) for this purpose since the amine group (NH_2) on TSC can interact with BNNS, while its amide/thiol (SH, sulfur containing) group can interact with copper[11], [12] and form a strong bridge. This functional molecule is very small compared to BNNS and copper crystals, which avoids hindrance of the thermal transport. After functionalization, the functionalized BNNS (f-BNNS) were incorporated into the copper matrix via a novel electrodeposition technique. f-BNNS suspended in the electrodeposition solution of copper were incorporated into the matrix via diffusion and convection. Once diffused, these linkers form a bond with copper atoms in the matrix and chemically link BNNS to copper grains. The concentration of the suspended f-BNNS was used to regulate the filler mass loading of the nanocomposites. The nanocomposites obtained were then characterized using scanning electron microscope (SEM), nanoindentor, diffusive laser flash (DLF), phase-sensitive transient thermoreflectance (PSTTR) and thermal mechanical analysis (TMA).

MATERIALS AND METHODS

Materials:

Hexagonal Boron Nitride, h-BN (98%, average particle size: 0.5 micron), was obtained from Lower Friction-M.K. IMPEX Corp, (Mississauga, Ontario, Canada). Sulphuric Acid (H_2SO_4, ACS reagent, 95.0-98.0%), Copper (II) Chloride ($CuCl_2$, 99%), Copper Sulfate pentahydrate ($CuSO_4.5H_2O$, ≥98%) and Poly (ethylene glycol) dithiol (average molecular weight (M_n) is 1500) were obtained from Sigma Aldrich (Saint Louis, MO). Thiosemicarbazide (TSC) (CH_5N_3S, >98%) and 1,3,4-Thiadiazole-2,5-dithiol ($C_2H_2N_2S_3$, >95%) were obtained from TCI America (Portland, OR). N-methlyl-2-pyrrolidone (C_5H_9NO, 99%) (NMP) was obtained from VWR (Radnor, PA). Copper bars were obtained from McMaster Carr (Elmhurst, IL) and aluminum substrate was obtained from Metals Depot (Winchester, KY). Silicon wafers (Silicon <100> P/Boron, >5000 ohm-cm, doubleside polish, <10 Angstrom R_a) were received from University Wafer (Boston, MA).

Functionalization of BNNS:

For BNNS functionalization, 1:10:100 ratios of BNNS, TSC and NMP were mixed in a flask and reacted at 170 °C in a nitrogen atmosphere for 36 hours and then, the mixture was dialyzed in 1:20 NMP solvent for 20 hours in two parts. The dialyzed material was centrifuged and the precipitate was collected. The precipitate obtained was washed in acetone and dried. This powder was used to analyze on X-ray photo spectrometry on Omicron XPS (Scienta Omicron GmbH, Taunusstein, Germany). Nuclear magnetic resonance spectra in solid state were obtained on the AVANCE-400 instrument. Infrared and Raman spectroscopies were obtained via a Shimadzu IR Prestige ATR-FTIR (Shimadzu Scientific Instruments Inc., Columbia, MD) and a high spectral resolution analytical Raman microscope (LabRAM HR Evolution, HORIBA, Ltd., Edison, NJ), respectively.

Synthesis of the Nanocomposite:

Synthesis of nanocomposite TIMs was achieved by electro-co-deposition of the f-BNNS in copper electrolyte solution on to aluminum sheets and silicon substrates. The aqueous electrolyte solution was prepared by 1M $CuSO_4.5H_2O$, 1.8 M H_2SO_4, a trace amount of $CuCl_2$, and various concentrations of f-BNNS. A pure copper sheet (>99%) and an aluminum/silicon substrate were connected to the anode and cathode, respectively. The electrical power source was a Nuvant Powerstat05 Potentiostat (Nuvant Systems Inc., Crown Point, IN). The deposition was carried out at a current density of 0 to 12 A/dm^2 and AC frequency of 950 Hz with 30% off time.

Characterization of the Nanocomposite:

Hardness and reduced elastic modulus of the nanocomposite TIM were measured via a Hysitron TI 950 Triboindenter (Hysitron Inc., Minneapolis, MN). A Berkovich tip with a well-defined geometry was used for indentation. A Modulated Q20 DSC (TA Instruments, New Castle, DE) was used to measure specific heat capacity. Thermal diffusivity measurements were performed via a DLF-1200 Laser Flash Diffusivity System (TA Instruments, New Castle, DE). The density of samples was determined gravimetrically. Further, PSTTR measurements were done at NREL, Colorado to determine thermal properties of the samples. The developed TIMs can be used in two configurations. First, the free-standing samples can be pressure-loaded between a heat sink and a heat source. In this configuration, the TIMs are reusable, but the contribution of the thermal contract resistance is increased. Second, the samples, via an adhesive layer, can be permanently bonded between a heat sink and a heat source, which was the purpose of the Al bonding layer. Regarding the specifics of the bonding, pure aluminum of 4.5 μm thickness was melted on top of a silicon substrate under argon atmosphere and rapidly transferred it on to the TIM surface which was coated on another silicon substrate (25.4 mm in diameter) to form a sandwich through the adhesion force under argon atmosphere. Finally, the system was cooled in room temperature to obtain a permanent diffusive bonding. The coefficient of thermal expansion was measured using a

thermal mechanical analyzer-TMA (TA Instruments, Newcastle, DE) with a built-in tensile test setup.

RESULTS AND DISCUSSION

Functionalization of BNNS:

This work seeks to develop chemically integrated metal-organic-inorganic nanocomposite materials. As a first step, investigation of the chemical reactions governing the formation of such integrated nanocomposite TIMs were carried out to confirm the reaction. The analysis of f-BNNS using Raman spectroscopy revealed the disappearance and major shifts at wavelengths 806 cm^{-1} (NH_2 wagging and CS stretching), 1008 cm^{-1} (NN stretching and CN stretching), 1172 cm^{-1} (NN stretching), 1526 cm^{-1} (NH bending), 1630 cm^{-1} (NH_2 bending), and 3258 cm^{-1} (NH_2 stretching) from the TSC spectra upon the reaction with BNNS (Fig. 1a).

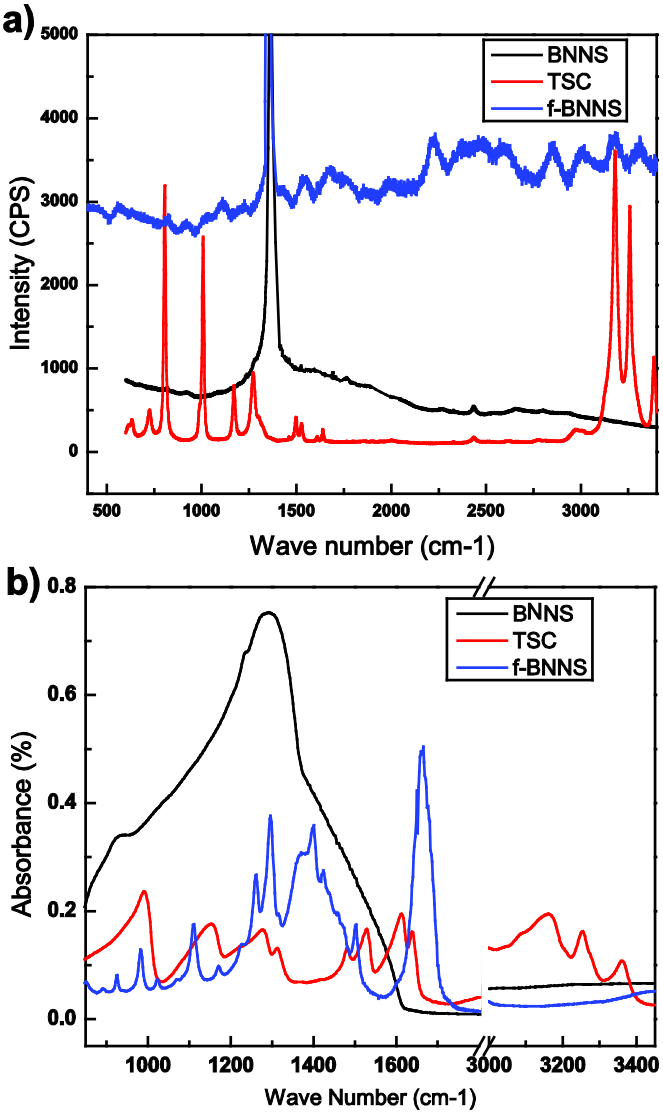

Fig. 1 (a) Raman spectrum of bare BNNS, pure TSC, and f-BNNS (On y-axis, CPS is counts per second). (b) FTIR spectrum of bare BNNS, pure TSC and f-BNNS supporting the changes observed in Raman spectroscopy.

The above observations indicate that the changes on TSC were on the amino group and also no significant changes occurred at the amide group. This implies the reaction is between the defective and edge B atoms of BNNS and amine of the TSC. These conclusions were also confirmed using FTIR spectroscopy as shown in Fig. 1b.

Nanocomposite Composition and Nanostructure:

Once the functionalization of BNNS was confirmed, nanocomposite TIMs were prepared at different mass loadings varying from 0 to 12 wt.%. In TIMs, the chemical linkage between copper and f-BNNS was confirmed using the XPS. XPS results as shown in Fig. 2 suggests that the pure copper has only one peak at 932.75 eV, but the nanocomposite material has two peaks - one at 932.75 eV and another at 934.65 eV. The new peak at 934.65 eV indicates an oxidized state and attachment of the thiol group (S) of TSC to copper. Also, it is important to note that, not all copper atoms are oxidized which indicates that the sulfur is not attached to all copper atoms.

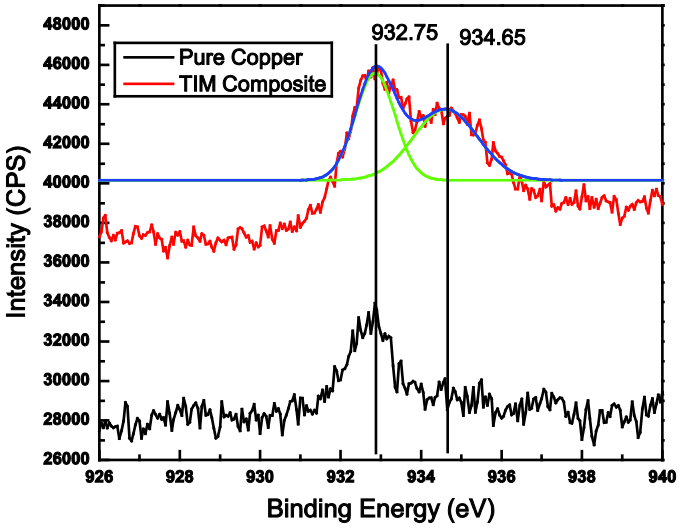

Fig. 2 XPS for pure copper and TIM nanocomposite. Two states of copper in the TIM (one pure and another oxidized) and just one state for pure copper suggest the oxidation of the copper in the TIM. Green lines indicate the expected peaks and the blue line is the combination of the green peaks. The fitting suits well with the obtained data.

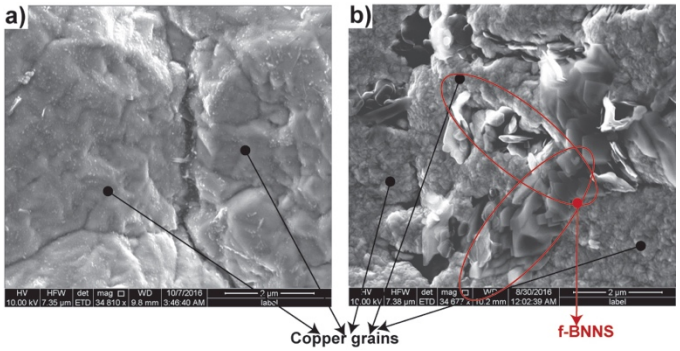

Fig. 3 (a) SEM micrograph of a pure copper deposited with same method shows no particles at grain boundaries.

(b) SEM micrograph of the TIM nanocomposite shows the presence of the f-BNNS in the grain boundaries in several locations

The attachment of f-BNNS to only few copper atoms has become clear in the SEM micrographs of the cross section of the TIMs. In Fig. 3b, it is observed that the f-BNNS occupy the grain boundary in contrast to no fillers in pure copper in Fig. 3a. This means only the copper atoms at grain boundaries are attached with sulfur and f-BNNS uniformly. The secondary ion micrographs support that the distribution of BNNS is uniform at a macroscopic level (not shown)[13].

Thermal Conductivity:

The presence of f-BNNS only at the grain boundaries helps to keep intact the intricate copper thermal transport network by maintaining copper–copper contacts and supports the thermal transport via electronic and phononic bandwidths. Though a few copper-copper contacts are shielded by f-BNNS, most of the contacts are still intact and only a few electronic transport channels are lost. However, due to the thermally conductive nature of the BNNS via phonons, a new phononic band width emerges. Anharmonic electron-phonon coupling at the copper-ligand-f-BNNS interface helps the transfer of heat via f-BNNS[14] across copper grains. Since the f-BNNS are edge functionalized, the phononic flux is restricted to only the in-plane direction. This is important because the BNNS possess high conductivity only in the in-plane direction. Also, due to the small size of the ligand, electron and phonon tunneling will take place to some extent to push the transport even further. Introduction of more f-BNNS in to the matrix will reduce the thermal conductivity. But, after certain filler loading, the grain boundaries are saturated by the f-BNNS and no new sites are left for the incoming f-BNNS. From this saturation point, no more loss of copper–copper contacts can take place and thus no loss of thermal transport. The implication of the discussion above is that the thermal conductivity of the nanocomposites reduces from 380 W/mK for pure copper to 220 W/mK for stabilized nanocomposite at around 5.5 wt% loading of f-BNNS as shown in Fig. 4.

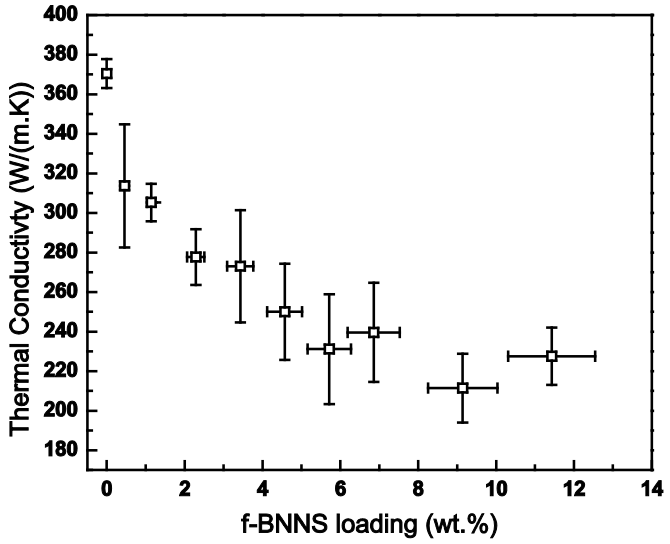

Fig. 4 Thermal conductivity of the TIM nanocomposites as a function of different weight loadings. Thermal conductivity stabilizes at 220 W/mK for approximately 5.5 wt.% loading of BNNS. Error bars represent one standard deviation of uncertainty.

The thermal conductivity is calculated according to the Equation 1:

$$k = \alpha . \rho . C_p \quad (1)$$

where α is the thermal diffusivity measure using DLF, ρ is the mass density measured using gravimetric analysis and C_p is the specific heat capacity measured using DSC.

Hardness:

Mechanically, the nanocomposites become softer due to the presence of organic molecules. In addition to the presence of the organic molecules, the nanostructure is also responsible for softening of the nanocomposite. Presence of filler materials at

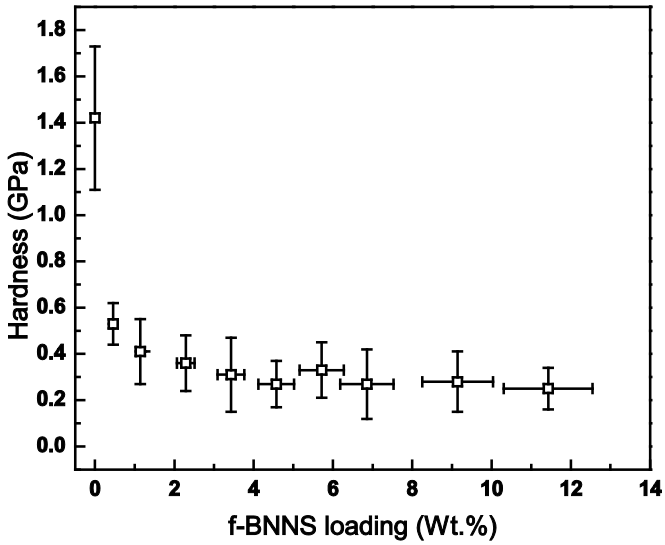

Fig. 5 Hardness of the TIM nanocomposites as a function of different weight loadings. Hardness stabilizes to 0.3 GPa around 4.5 wt.% loading. This is 4 times softer than pure copper. Error bars represent one standard deviation of uncertainty.

the grain boundaries provide periodic cushions for the matrix – which makes it soft. Fig. 5 shows the reduction of hardness from 1.42 GPa to 0.33 GPa for the 6 wt.% loading TIM. Nanoindentor was used to measure the hardness of the composite since, it simulates the asperities of the mating heat sink and heat source. The TIM with 4.5 wt.% percentage loading is around 4 times softer than pure copper. After the saturation point as discussed above, the f-BNNS in the system will make it difficult for the copper matrix to hold well due to excess stacking at the grain boundaries - leading to the breaking of the copper grain bonding.

Thermal Resistance:

Overall thermal resistance is a function of bulk thermal conductivity, thickness of the TIM layer and the interfacial thermal contact resistance. Thermal resistance measurements were carried out using the PSTTR technique. In this technique, two lasers are used to study the thermal properties (thermal resistance and thermal conductivity) of a multilayer structure. Phase shift is measured from the modulated pump laser and

the corresponding probe laser waveform. Fitting the phase shift with the theoretical heat transfer model, thermal properties can be accurately determined[15]. Measurements were made in a sandwich configuration as shown in Fig.6. These TIMs were permanently bonded through the diffusion bonding via Al under adhesive loading. This is the favorable route to pursue for fragile electronic components. The effect of pressure is better suited to be studied for the reusable samples that are mechanically fastened between a heat sink and a heat source. While our materials can also be used in this fashion, we have not tested the thermal resistance as a function of pressure yet, which will be a potential future study. Therefore, when developing the heat transfer model, the interfacial layer was considered to have two solid layers (hybrid nanocomposite and aluminum) and three interfaces. Contact resistance between the hybrid nanocomposite and silicon substrate (R_{34}) was already identified by the characterization of the single-sided samples. With prior information on the bulk thermal conductivity of the hybrid nanocomposite, and the contact resistance between the hybrid nanocomposite and silicon substrate, only the contact resistances of the other two interfaces (Si-Al (R_{12}) and Al-nanocomposite (R_{23})) are needed to be determined for the bonded samples. Hence, the four critical unknown parameters were acquired from two independent fitting procedures, and the reliability of the results was consequently very good. By summing the bulk thermal resistances and interfacial contact resistances, the total thermal resistance of the interfacial layer was calculated. Thermal resistance of the interface of the TIM with the silicon substrate and also the total thermal resistance of the nanocomposite TIM (4.5 wt% loading) were measured at 30 µm and 50 µm BLT in a sandwiched configuration. Because the PSTTR thermal characterization combines both experiment and regression fitting, the uncertainty analysis is more complex. The experiments were completed using an automated data acquisition system that was built to collect the amplitude and phase extracted from the lock-in amplifier. For each frequency generated from the function generator, the sampling time was 60 seconds and the sampling rate was 10 Hz. Then, the average value of 600 samples that were collected was recorded as the amplitude and phase associated with this frequency. The data acquisition system is estimated to have about 5 degrees random uncertainty. The lock-in amplifier has a systematic uncertainty of about 1 degree. In addition, the regression process to analyze the experimental data also is an important source of error. The reason is that when fitting the experimental data and theoretical results, other modeling parameters, known or unknown, are applied with different levels of uncertainty.

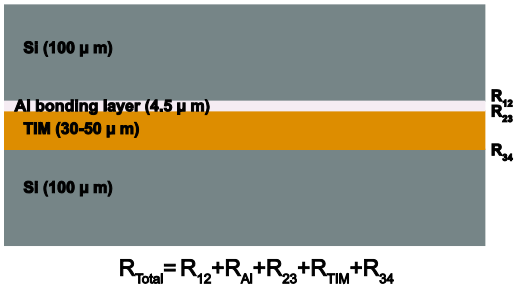

Fig. 6 Sandwich configuration for the thermal resistance measurements used in the PSTTR technique.

Here, the uncertainty of the to-be-determined parameters is estimated from the uncertainties in the modeling parameters[16]. After determining the best fit, each of the modeling parameters is perturbed by a small quantity (its uncertainty) and the regression process is repeated to find the new fitted value of the to-be-determined unknowns. Then the difference between the new and old values is the uncertainty from the fitting process used to determine the unknown parameters. Using this methodology and combining fitting uncertainty with the measurement uncertainty (random and systematic uncertainty), the uncertainty of thermal conductivity at 95% confidence level is calculated to be 27%, while that for the R_{12} and R_{23} is 31% and 39%, respectively. This leads to an uncertainty of about 16% for the total thermal resistance. We see an extremely low thermal contact resistance (R_{34}) of 0.08 mm^2K/W and total thermal resistance of 0.38±0.06 mm^2K/W for 30 µm BLT and 0.56±0.10 mm^2K/W for 50 µm BLT.

Coefficient of Thermal Expansion:

TMA measurements revealed that the CTE of the nanocomposite TIM at 12 wt.% loading is 11 ppm/K compared to 17 ppm/K of pure copper as shown in Fig. 7. This value of CTE is desirable since the most common chip material – silicon - has a CTE of 2.7 ppm/K and the CTE of our TIMs lie in between the CTE of silicon and common heat sink materials (aluminum (22 ppm/K) and copper (17 ppm/K)). Commonly used indium or epoxy-based TIMs, which have a typical CTE of 20 ppm/K and 30 ppm/K, respectively, are associated with a higher risk of thermal stress due to a large CTE-mismatch between the heat source and heat sink junctions. As such, the nanocomposite TIMs can reduce mechanical stress due to CTE-mismatch and aid the long-term reliability. We subjected the samples to 60 cycles going from a temperature of 25°C to 100°C, where most electronic devices are expected to operate. We notice no significant drop in thermal conductivity. The thermal conductivity for a 4.5 wt.% sample changed from 250 W/mK to 220 W/mK - which corresponds to a change of thermal resistance from 0.38 mm^2K/W to 0.4 mm^2K/W for a sample with 30-µm BLT. Performing long-term cycling tests to understand the role of CTE mismatch is one of the future topics that we plan to focus on.

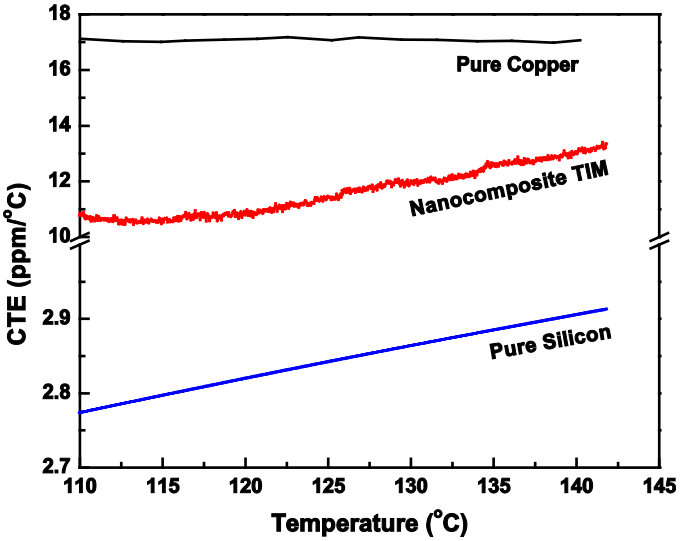

Fig. 7 CTE values for the pure silicon, pure copper and nanocomposite TIM compared in the range of 110 °C - 140 °C. It is very clear from the graph that the CTE of the TIM makes it a perfect bridging material between silicon and copper from the perspective of handling thermal stresses.

To put the obtained results into a perspective, we compare the total thermal resistance values of various types of TIMs with our nanocomposite TIMs described in this work in Fig. 8. It is clear that the new nanocomposite TIMs significantly outperforms the contemporary TIMs, pushing the limits of thermal management to the next level. We see that the nanocomposite TIM produced in this study has an average thermal resistance value of 0.56 mm^{2}K/W for 50 μm that has outperformed all other TIMs. All the values for thermal resistances given in the Fig. 8 are for a BLT range of 25-50 μm.

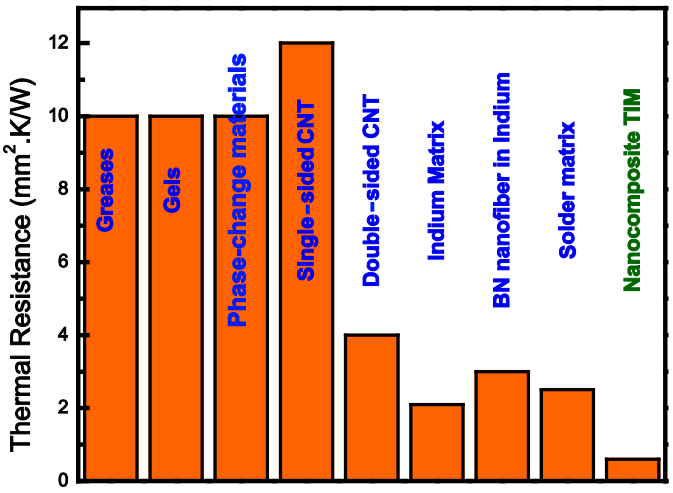

Fig. 8 Comparison of resistances for different TIM classes as taken from Narumanchi et al.[17], Indium matrix[18], BN nanofiber in indium[19], solder matrix nanopolymer [20] and this work (Nanocomposite TIM).

CONCLUSION

We synthesized and demonstrated a new class of nanocomposite TIMs that outperformed current state-of-the-art TIMs. The copper-based TIMs developed in this work have 60% of the thermal conductivity of the pure copper, while being four times softer than copper. This makes the new TIM soft and a thermally-conducting material. In addition, the developed TIM has a CTE value between that of silicon and copper - which will help it act as a bridge between the mating surfaces and handle thermal stresses very well. Also, the TIM has a total thermal resistance value of 0.38 and 0.56 mm^{2}K/W for a BLT of 30 and 50 μm, respectively, which is a significant improvement compared to previous classes of TIMs of comparable BLT. Further investigating this class of nanocomposite TIMs will likely result in even more improvements to these values, and they will help improve the thermal management in power-dense electronic systems in the near future.

ACKNOWLEDGMENTS

This research was funded by the Defense Advanced Research Projects Agency (DARPA) of the U.S. Department of Defense. The views, opinions and/or findings expressed are those of the authors and should not be interpreted as representing the official views or policies of the Department of Defense or the U.S. Government. M.A acknowledges funding from NSF Grant 1559627.

REFERENCES

[1] G. Pernot *et al.*, "Precise control of thermal conductivity at the nanoscale through individual phonon-scattering barriers.," *Nat. Mater.*, vol. 9, no. 6, pp. 491–495, 2010.

[2] A. Yu, P. Ramesh, X. Sun, E. Bekyarova, M. E. Itkis, and R. C. Haddon, "Enhanced Thermal Conductivity in a Hybrid Graphite Nanoplatelet - Carbon Nanotube Filler for Epoxy Composites," *Adv. Mater.*, vol. 20, no. 24, pp. 4740–4744, Dec. 2008.

[3] X. Wang, Y. Hu, L. Song, H. Yang, W. Xing, and H. Lu, "In situ polymerization of graphene nanosheets and polyurethane with enhanced mechanical and thermal properties," *J. Mater. Chem.*, vol. 21, no. 12, pp. 4222–4227, 2011.

[4] S. Stankovich *et al.*, "Graphene-based composite materials.," *Nature*, vol. 442, no. 7100, pp. 282–286, 2006.

[5] M. J. Biercuk, M. C. Llaguno, M. Radosavljevic, J. K. Hyun, A. T. Johnson, and J. E. Fischer, "Carbon nanotube composites for thermal management," *Appl. Phys. Lett.*, vol. 80, no. 15, pp. 2767–2769, 2002.

[6] H. Jiang, K. Moon, Y. Li, and C. P. Wong, "Surface functionalized silver nanoparticles for ultrahigh conductive polymer composites," *Chem. Mater.*, vol. 18, no. 13, pp. 2969–2973, 2006.

[7] G. K. White, "Thermal expansion of reference materials: copper, silica and silicon," *J. Phys. D: Appl. Phys.*, vol. 6, no. 17, p. 2070, 1973.

[8] A. Bar-Cohen, K. Matin, and S. Narumanchi, "Nanothermal Interface Materials: Technology Review

and Recent Results," *J. Electron. Packag.*, vol. 137, no. 4, p. 40803, 2015.
[9] Y. Lin and J. W. Connell, "Advances in 2D boron nitride nanostructures: nanosheets, nanoribbons, nanomeshes, and hybrids with graphene," *Nanoscale*, vol. 4, no. 22, p. 6908, 2012.
[10] L. Lindsay and D. a. Broido, "Enhanced thermal conductivity and isotope effect in single-layer hexagonal boron nitride," *Phys. Rev. B*, vol. 84, pp. 1–6, 2011.
[11] P. E. Laibinis and G. M. Whitesides, "Self-Assembled Monolayers of n-Alkanethiolates on Copper Are Barrier Films That Protect the Metal against Oxidation by Air," *J. Am. Chem. Soc.*, vol. 114, pp. 9022–9028, 1992.
[12] Y. S. Shon, G. B. Dawson, M. Porter, and R. W. Murray, "Monolayer-protected bimetal cluster synthesis by core metal galvanic exchange reaction," *Langmuir*, vol. 18, no. 10, pp. 3880–3885, 2002.
[13] C. Yegin *et al.*, "Metal-Organic-Inorganic Nanocomposite Thermal Interface Materials with Ultra-Low Thermal Resistances," *ACS Appl. Mater. Interfaces*, p. acsami.7b00093, Feb. 2017.
[14] P. J. O'Brien *et al.*, "Bonding-induced thermal conductance enhancement at inorganic heterointerfaces using nanomolecular monolayers.," *Nat. Mater.*, vol. 12, no. 2, pp. 118–22, 2013.
[15] J. A. Malen, K. Baheti, T. Tong, Y. Zhao, J. A. Hudgings, and A. Majumdar, "Optical Measurement of Thermal Conductivity Using Fiber Aligned Frequency Domain Thermoreflectance," *J. Heat Transfer*, vol. 133, no. 8, p. 81601, 2011.
[16] X. Feng, C. King, D. Devoto, M. Mihalic, and S. Narumanchi, "Investigation of thermal interface materials using phase-sensitive transient thermoreflectance technique," *IEEE Intersoc. Conf. Therm. Thermomech. Phenom. Electron. Syst., 14th* ., pp. 1296–1307, 2014.
[17] S. Narumanchi, M. Mihalic, K. Kelly, and G. Eesley, "Thermal interface materials for power electronics applications," *IEEE Intersoc. Conf. Therm. Thermomech. Phenom. Electron. Syst., 11th*.,pp. 395–404, 2008.
[18] S. Sun, S. Chen, X. Luo, Y. Fu, L. Ye, and J. Liu, "Mechanical and thermal characterization of a novel nanocomposite thermal interface material for electronic packaging," *Microelectron. Reliab.*, vol. 56, pp. 129–135, 2015.
[19] X. Luo *et al.*, "Novel thermal interface materials: boron nitride nanofiber and indium composites for electronics heat dissipation applications," *J. Mater. Sci.: Mater. Electron.*, vol. 25, no. 5, pp. 2333–2338, Mar. 2014.
[20] C. Zandén, X. Luo, L. Ye, and J. Liu, "A new solder matrix nano polymer composite for thermal management applications," *Compos. Sci. Technol.*, vol. 94, pp. 54–61, 2014.